Geophysical Journal (1988) **94**, 367–376

Deflection of plumes by mantle shear flow: experimental results and a simple theory

Mark A. Richards* and Ross W. Griffiths
Research School of Earth Sciences, Australian National University, Canberra, A.C.T. 2601, Australia

Accepted 1988 January 14. Received 1988 January 11; in original form 1987 October 20

SUMMARY

Linear hotspot tracks indicate relative motion between some hotspot sources and the overlying lithosphere. In order to better understand the effects of plate motions and mantle convection on mantle plumes and associated hotspots, we consider the path of a continuous plume of buoyant material in a shear flow. Laboratory experiments show that steady plumes bent over by a linear velocity profile follow parabolic trajectories. Plume trajectories are also shown to evolve quadratically in time toward a new steady shape after a change in the ambient flow. A remarkably simple description of plume dynamics provides good agreement with the experimental data: the plume trajectory is determined by the combination of horizontal advection by mantle flow and vertical rise according to a modified Stokes law. These results are applied to some idealised examples which demonstrate effects of depth-dependent mantle viscosity and return flow. At least some mantle plumes are likely to be sufficiently robust that they remain close to vertical and, therefore, stable.

Key words: hotspots, mantle convection, plumes, shear flow

INTRODUCTION

Plumes of hot, buoyant and geochemically distinct material rising from deep in the mantle are the likely cause of major mid-plate volcanoes or hotspots such as Hawaii and Iceland (Morgan 1972; 1982). Hotspot tracks such as the Hawaiian–Emperor seamount chain and the Line Islands–Tuamotu chain imply relative motion between some hotspot sources and the oceanic lithosphere, hence a gradient of horizontal velocity with depth. Relative motions of hotspots are smaller by at least a factor of 2 or 3 than relative oceanic plate motions, although the assumptions of a fixed or absolute hotspot reference frame (often used in global plate reconstructions) is questionable (Molnar & Stock 1987). To whatever degree it exists, the apparent independence of hotspot locations from plate motions implies that the boundary layer or thermal sources responsible for hotspots are not strongly coupled to convection associated with the lithospheric plates.

As plumes rise through the mantle, they will be deflected from the vertical by the shear flow and return flow due to plate motions. However, the magnitude of this deflection will depend upon the strength of the plume. A large plume might rise almost vertically through the mantle. A weaker plume could be deflected so that its surface expression (hotspot) is displaced horizontally a large distance from its source. If a plume or conduit is bent to angles greater than about 60° from the vertical, conduit instabilities result. Laboratory experiments with weak plumes in a shear flow show that these instabilities break up the plume into discrete blobs or diapirs which rise independently (Skilbeck & Whitehead 1978; Whitehead 1982).

Plume instability due to velocity gradients in the upper mantle or asthenosphere was initially suggested as an explanation for episodicity of volcanism and discretization of hotspot tracks into a chain of volcanic centres, or islands. This hypothesis was dismissed when further laboratory experiments (Whitehead 1982; Olson & Singer 1985) provided unreasonable scalings for the size and periodicity of diapirs formed on a sheared conduit. Instead, Olson & Nam (1986) and Griffiths, Gurnis & Eitelberg (1987) show that only very large diapirs of diameter 400–500 km can explain the topographic swells surrounding hotspots. We believe the evidence for such enormous, discrete mantle blobs to be very weak, at least for Hawaii. However, the issue of discrete blobs versus continuous (though not necessarily steady) plumes remains an open question in need of more experimental, theoretical, and observational work.

Evidence from hotspot tracks for the interactions of plumes with plate motions offers a rich variety of natural experiments. As examples, the Galapagos hotspot has passed through an active spreading ridge, and Iceland imposes a very regular trend of geochemical anomalies along the slow-spreading Reykjanes Ridge (e.g. Poreda, Craig & Schilling 1980) with respect to which it remains almost stationary. The most spectacular feature, however, is the sharp bend in the Hawaiian–Emperor seamount chain due, apparently, to an abrupt change in Pacific plate motion

* Present address: Department of Geological Sciences, University of Oregon, Eugene, Oregon 97403, USA.

about 40 Ma. This bend has a radius of curvature of 200 km or less, implying a very rapid adjustment of the plume to the more recent direction of plate motion. We believe this to be a key piece of information constraining the size and configuration of the plume beneath Hawaii.

Although conduit instabilities and conditions for their formation have been investigated in detail by Whitehead (1982), the deflection and adjustment of a continuous conduit in a shear flow has received little attention. We were motivated to study the deflection of stable, continuous plumes in order to understand the Hawaiian–Emperor bend: it did not seem reasonable that a plume deflected a large distance horizontally (say a large fraction of the upper mantle depth) could adjust so rapidly. Our subsequent work strongly supports this view, and we present the results in two separate papers.

In this paper we address the physics of deflection of a steady, continuous plume in a shear flow. Laboratory experiments are shown to verify a remarkably simple and straightforward theory describing plume trajectories, which can be applied to any prescribed shear/return flow due to plate motions. In a following paper (in preparation) we discuss the detailed application of our results to observations from the Hawaiian–Emperor island and seamount chain.

A SIMPLE HYPOTHESIS

The trajectory (or shape) of a mantle plume from its source involves two competing effects: the tendency of the plume to rise vertically and the tendency of the plume to be advected along with the background mantle flow. Advection of the plume must be determined from constraints on the larger scale flow in the mantle, e.g. by continuity of viscous stress associated with shear flow beneath moving lithospheric plates. The main aim of our experiments is to characterize the vertical rise component of the plume due to its own buoyancy in the presence of a given shear flow.

We hypothesize that each plume element has a characteristic rise velocity which can be added vectorially to the background flow velocity field in order to determine its trajectory. Further, we hypothesize that this rise velocity can be written as a modified Stokes velocity

$$v_s = \frac{k\Delta\rho g a^2}{\eta}, \tag{1}$$

where $\Delta\rho$ is the density contrast between the plume and the mantle, g the gravitational acceleration, a the plume radius, η the mantle viscosity, and k is a constant to be determined experimentally. Note that our hypothesis applies to plume or conduit elements, *not* to fluid parcels which flow through the plume. It is to be expected that fluid velocities within the plume are, at least for low viscosity plumes, much greater than the Stokes velocity of the conduit itself.

The form of (1) is that of the Stokes formula for the rise of a buoyant sphere or cylinder, except for a numerical factor allowing for the differing geometry of a plume. (Note that the validity of (1) applied to conduits carrying buoyant fluid, possibly of very low viscosity, is not obvious. Indeed, Skilbeck & Whitehead (1978) attempted to characterise the rise of an inclined plume in terms of a rigid cylinder whose axis was inclined at an angle to the vertical.) Theoretical prediction of this numerical factor an arbitrary plume is difficult. Hence we aim to determine the constant k (and whether it is, indeed, a constant) experimentally. We can make two specific predictions using equation (1) which serve to clarify our hypothesis and which guide the experimental work.

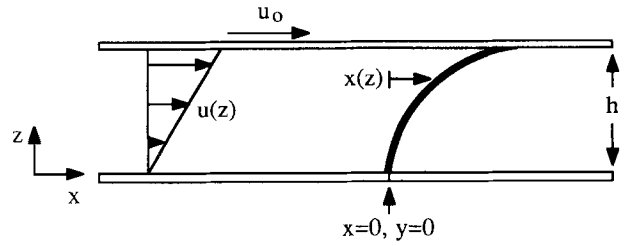

Figure 1. Diagram of a simple shear flow and a plume advected horizontally from its source.

Case 1: Steady-state deflection. Consider a plume rising from a fixed source at the rigid base of a tank into a uniform fluid of viscosity η. Let the fluid be in a state of shear, driven by a rigid plate at the top moving horizontally with constant velocity u_0 (see Fig. 1). The horizontal velocity in the fluid must increase linearly from zero at the bottom of the tank to u_0 at the moving top plate:

$$u = u_0 \frac{z}{h}, \tag{2}$$

where h is the depth of the fluid. The plume will be bent as sketched in Fig. 1. We ask: What is the steady-state profile after both the plume and plate motion have been turned on for a long time? The horizontal position, x, of a plume element at height z is given by

$$x(t) = \int_0^{t(z)} u(z)\, dt, \tag{3}$$

where $t(z)$ is the time for a plume element to rise to height z. This vertical rise time is the height z divided by the modified Stokes rise velocity which, according to our hypothesis above, is a constant v_s:

$$t(z) = \frac{z}{v_s} \quad \text{or} \quad dt = \frac{dz}{v_s}. \tag{4}$$

Substituting (4) into (3) we obtain

$$x(z) = \int_0^z \frac{u}{v_s}\, dz. \tag{5}$$

Upon integration and substitution from (1):

$$x(z) = \frac{\eta}{kg\,\Delta\rho a^2} \frac{u_0}{h} \frac{z^2}{2}. \tag{6}$$

In non-dimensional form

$$\frac{x(z)}{h} = \frac{\eta u_0}{2kg\,\Delta\rho a^2} \left(\frac{z}{h}\right)^2. \tag{7}$$

Equation (7) predicts that the steady state profile of the plume in a simple shear flow should be parabolic. Solving

(7) for k,

$$k = \frac{h}{x(z)} \frac{\eta u_0}{2g\,\Delta\rho a^2} \left(\frac{z}{h}\right)^2, \tag{8}$$

gives an equation which allows us to determine the value of the constant for various combinations of experimental parameters. The value of k is likely to be dependent upon the viscosity of the plume itself. However, as long as the plume viscosity is much less than the tank fluid viscosity, the variation with viscosity should be small. We also note here an obvious oversimplification which is discussed more fully later: because the inclination of the plume is a function of height, the plume radius, a, is not constant (Whitehead 1982). Thus for large excursions, $\frac{x(z)}{h}$, equations (7) and (8) may have to be modified.

Case 2: Transient adjustment. We also wish to know how the plume evolves in time when the shear flow is altered. Consider a plume bent to its steady-state configuration as in Fig. 1. If the horizontal plate motion is suddenly turned off, how does the plume profile relax toward the vertical? If our hypothesis leading to (1) is correct, then the conduit at $x(z, t)$ should relax to position $x(z, t + \Delta t)$ (Fig. 2) as the plume element at $x(z - \Delta z, t)$ rises the distance Δz. This behaviour is expressed in the difference equation

$$x(z, t + \Delta t) - x(z, t) = x(z - \Delta z, t) - x(z, t) \tag{9}$$

or

$$\frac{\partial x}{\partial t} = \frac{-\partial z}{\partial t} \frac{\partial x}{\partial z}. \tag{10}$$

According to our hypothesis, $\frac{\partial z}{\partial t} = v_s$ so that

$$\frac{\partial x}{\partial t} = -v_s \frac{\partial x}{\partial z}. \tag{11}$$

This is a simple one-dimensional wave equation with solutions of the form $x(z, t) = x(z - v_s t, 0)$. For a plume stretched out to the profile given by (6), the horizontal displacement will 'relax' according to

$$x(z, t) = \frac{u_0}{2hv_s}(z - v_s t)^2, \tag{12}$$

where t is the time after plate motion ceases. For an initially vertical plume, the horizontal displacement will 'stretch' after plate motion commences according to

$$x(z, t) = \frac{u_0}{2h} t(2z - v_s t). \tag{13}$$

Equations (12) and (13) show that the plume adjusts to its new steady state in the time $t = z/v_s$. Hence the adjustment time for a plume in a simple shear flow increases linearly with height, z, from the source.

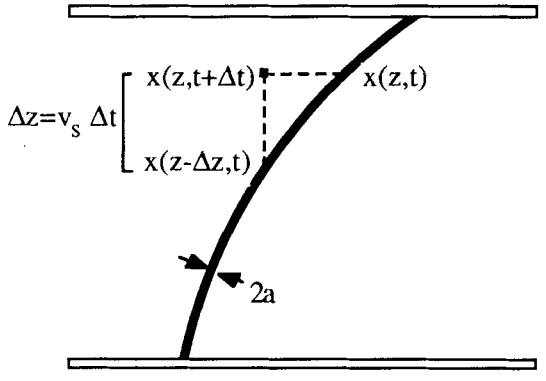

Figure 2. Sketch of a displaced plume, showing the coordinate notation used to analyse the motion of a plume element.

EXPERIMENTAL METHODS

A simple shear flow was generated using the cylindrical, plexiglass tank illustrated in Fig. 3. A lid with a radius about 5 mm less than the inside diameter of the tank was fitted on an axle so that it could rotate freely. The lid was rotated at a constant rate by a small electric motor via a pulley system (not shown). The distance between the bottom of the lid and the bottom of the tank (about 10 cm) was deliberately made small with respect to the tank diameter (60 cm) so that flow mid-way between the axis and sidewall would closely approximate the linear increase with depth of a simple shear flow (see Fig. 1). The plume was injected through a small opening at the bottom of the tank 12 cm away from the axis and 18 cm from the sidewall. The plume fluid was fed through a plastic tube from an elevated reservoir, and the flow was controlled by a simple in-line needle valve. The tank fluid was almost pure glycerol (with some contaminating water) of density 1.26 g/cm^3 and kinematic viscosity 790 cS. Plume fluids consisted of mixtures of glycerol and water having lower densities and viscosities than the tank fluid.

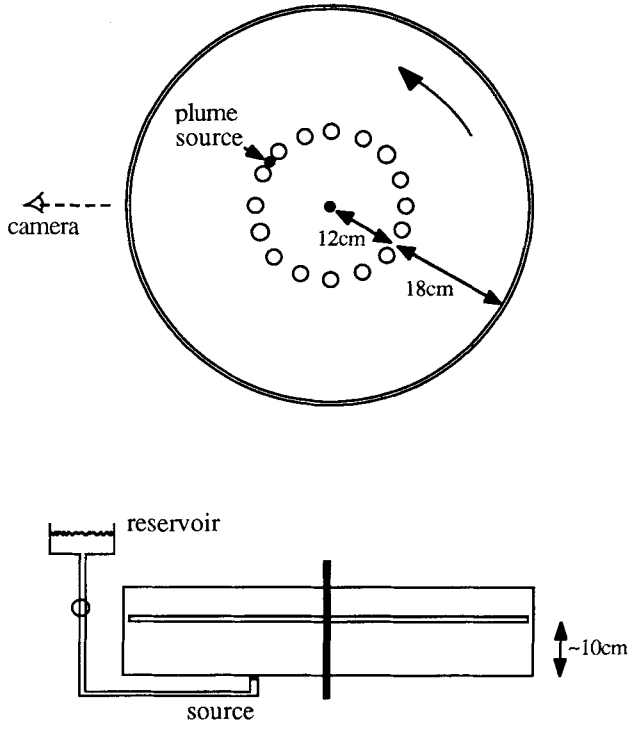

Figure 3. The laboratory apparatus in plan and side view.

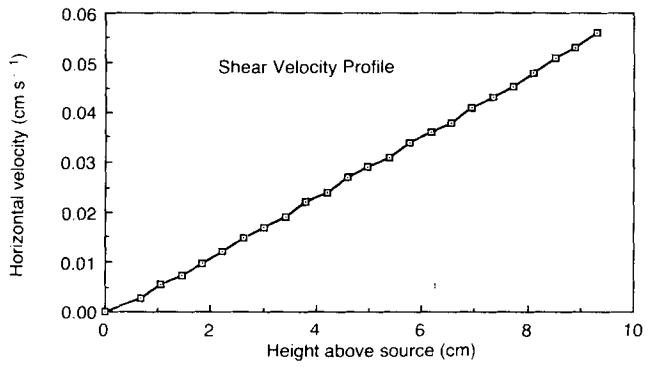

Figure 4. The measured velocity profile over the depth of the tank.

We anticipated one practical problem: as experiments proceeded, buoyant low viscosity plume fluid would collect beneath the rotating lid and reduce coupling between the lid and the tank fluid. This was overcome to a large extent by cutting holes in the lid at the same radius as the plume source and filling the tank to a height above the top of the lid (see Fig. 3). As the top of the plume was wrapped around the axis at a fixed radius by the shear flow, the plume fluid would escape through the holes to the surface of the glycerol above the lid. This modification worked well, with only slight effects on the rise of the plume fluid within 1 cm of the lid—where the plume approached solid portions of the lid it rose more slowly than where it approached a hole.

Each experiment was recorded by taking photographs through the side of the tank at regular time intervals with a 35 mm camera. Measurements were made by projecting the negative against a screen, tracing the plumes onto graph paper, and digitizing the plume profiles. The vertical and horizontal scales were set along the cylindrical surface at the source radius by photographing a plastic cylinder, radius 12 cm, placed inside the tank. This cylinder had regularly spaced vertical and horizontal lines which defined the length scale along the plume trajectories.

The shear velocity profile in the tank at the position of the plume was measured as follows: a very narrow plume, dyed red, was injected and brought to a steady state with no plate motion, i.e. a vertical plume. Its position was recorded photographically. Then the plate motion was turned on and another photo was taken a short time (30 s) later. Since the plume was very weak, it offered almost no resistance to being advected horizontally by the shear flow, and its displacement between the two photographs gave the shear velocity profile directly. The velocity profile obtained is shown in Fig. 4, and it is indeed very close to linear. The extrapolated velocity at the bottom of the lid is 0.064 cm/s (at radius 12 cm), which agrees with that determined by measuring the rotation rate of the lid. Therefore, our attempt to create a simple shear flow between the top and bottom of the tank was successful.

In order to fully test the theory for plume deflection by shear flow, equations (6) and (13) must be shown to hold for a single constant value of k regardless of the plume parameters. We varied both the plume radius, a, and the density contrast, $\Delta\rho$, in the experiments that follow. The relevant parameters for each experiment are given in Table 1. The radius was varied over a range sufficient to span steady state plume shapes from those having very little deflection up to those having very large deflections (>60° from the vertical). Plume radius was varied by controlling the plume flow rate from its reservoir (see Fig. 3). The plume fluids were mixtures of glycerol and water plus a small amount of red dye: 80% glycerol +20% water by volume in experiments A1–A3, and 90% glycerol +10% water for B1–B3. The plume viscosities were estimated from standard mixing curves and were much less than the tank fluid viscosity.

The plume radii were measured from photographs of the steady, vertical plumes without plate motion. The plume radius in the middle of the tank was slightly smaller (but by less than 10 per cent) than near the top and bottom, and the values given in Table 1 are an average over four evenly-spaced heights above the source. Some uncertainty in radius measurement arises due to the refractive index contrast between plume and tank fluid: light is refracted at the edges of the plume, and the edge itself appears fuzzy in the photographs. We estimate an uncertainty in plume diameter of about ±0.3 mm. This is probably the largest source of error in the experiments.

EXPERIMENTAL RESULTS

Two series of experiments were run (A and B) with different density (and viscosity) contrasts. For each series, three different plume radii were used. For experiment A2 (see Table 1) several plume profiles are shown in Fig. 5. These photographs show the plume before the plate motion is turned on (5a), at a short time after plate motion is started (5b), at a steady-state (>240 s) of horizontal deflection (5c),

Table 1. Experimental parameters for six plumes, along with the values of the modified Stokes constant k found by fitting the steady state trajectories of plumes in a linear velocity profile.

Exp.#	h	η_{plume}/η_{tank}	$\Delta\rho(gcm^{-3})$	2a(cm)	k
A1	10.5cm	0.07	0.051	(.16)	(0.79)
A2	"	"	"	.32	0.54
A3	"	"	"	.60	0.55
B1	9.5cm	0.25	0.026	.34	0.56
B2	"	"	"	.55	0.52
B3	"	"	"	.83	0.51

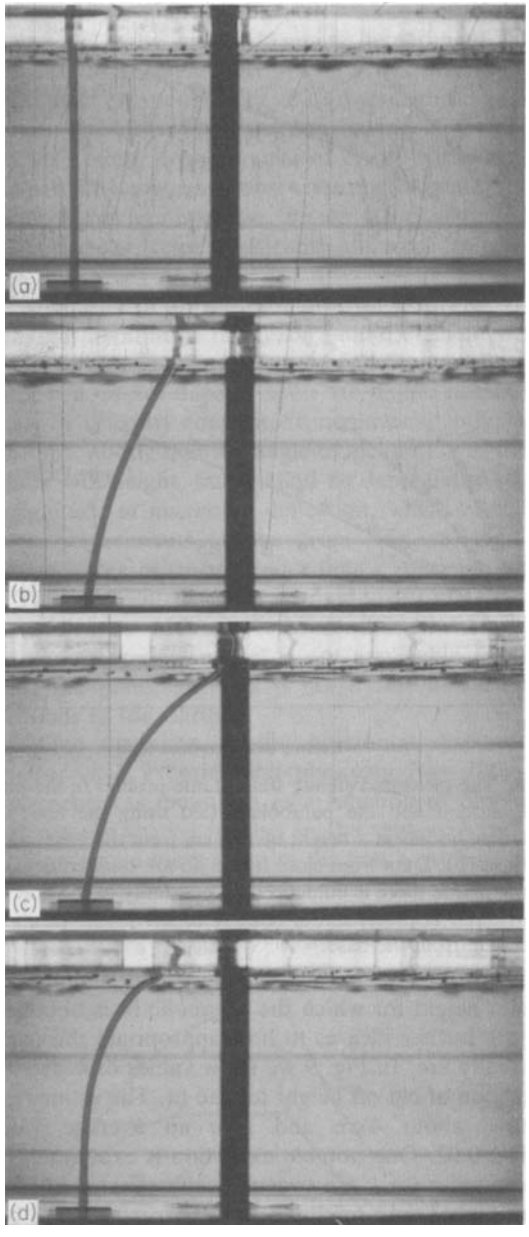

Figure 5. Photographs showing the shape of the plume in run A2 (a) before plate motion is begun; (b) 60 s after plate motion began; (c) in its steady state 240 s after motion began; and (d) 60 s after plate motion is stopped. The plume eventually becomes vertical again. The solid vertical bar is the axial shaft supporting the lid.

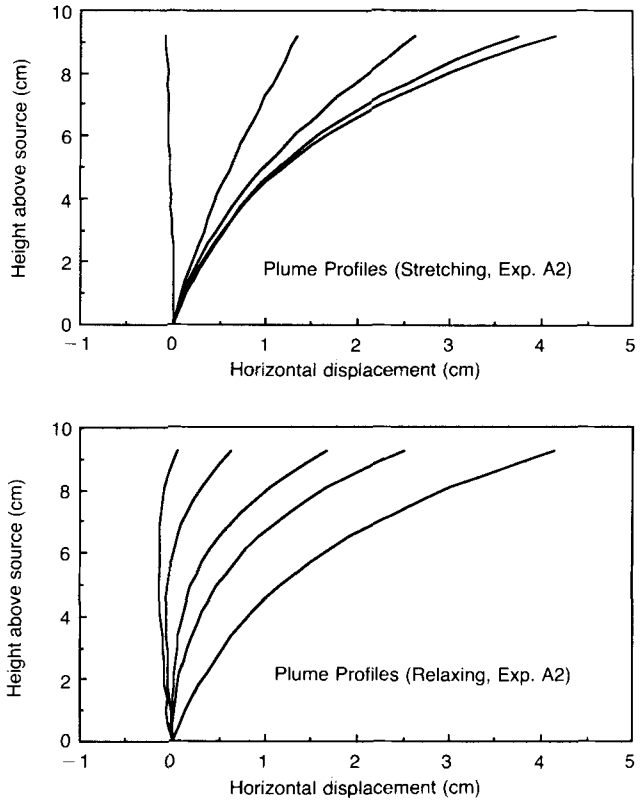

Figure 6. The shape of the centre line of the plume in run A2 at various times (a) after the plate motion began ('stretching') and (b) after the plate motion stopped ('relaxing'). In (a) the plume is initially close to vertical and is progressively displaced toward its final steady shape. In (b) the plume relaxes toward the vertical.

and at an intermediate time after the plate motion is turned off (5d). Such photographs constitute the basic data used here. Note that photos 5b and 5d are quite different: in 5d the upper parts of the plume have relaxed slowly compared to the lower parts leading to greater curvature, while in 5b the plume deflection is initially linear with height. Equation (13) shows that this is to be expected, predicting that the upper part of the plume is slower to adjust toward either of the two steady states (plate motion on or off). We also note that the plume is stable at all times, including when bent over to the maximum extent. The dependence of adjustment time τ upon z is better illustrated in Figs 6(a),(b), where profiles of the centerline of the plume are shown at the complete set of time intervals. The 'stretching' profiles show deflection after plate motion is turned on, and the 'relaxing' profiles show deflection after plate motion is turned off.

Steady-state deflection profiles are shown for experiments A1–A3 in Fig. 7. The deflection decreases with the square of increasing plume radius, and all three profiles are approximately parabolic as anticipated in (6). Values for the constant k, defined in (1), can be estimated by fitting parabolas to the x versus z data for the steady-state displacement profiles.

Referring to (6) we wish to determine k' for each plume such that the form

$$x(z) = k'z^2 \tag{14}$$

gives an optimum fit. Here $k' = \dfrac{\eta u_0}{2kg\,\Delta\rho a^2 h}$ so that a determination of k' results in a determination of k with all the other parameters known for each experiment.

One practical modification to (14) is required to estimate k accurately. This results from the fact that the plume must undergo a rapid adjustment as it enters the tank from the small (2 mm diameter) source hole. Over a small vertical distance the plume widens and reaches a constant diameter. We estimate this distance to be less than 1.5 cm in our experiments, and we have arbitrarily taken a 'virtual' plume source to be at a height of 1.4 cm above the tank bottom. A review of (3)–(6) shows that this is a trivial modification

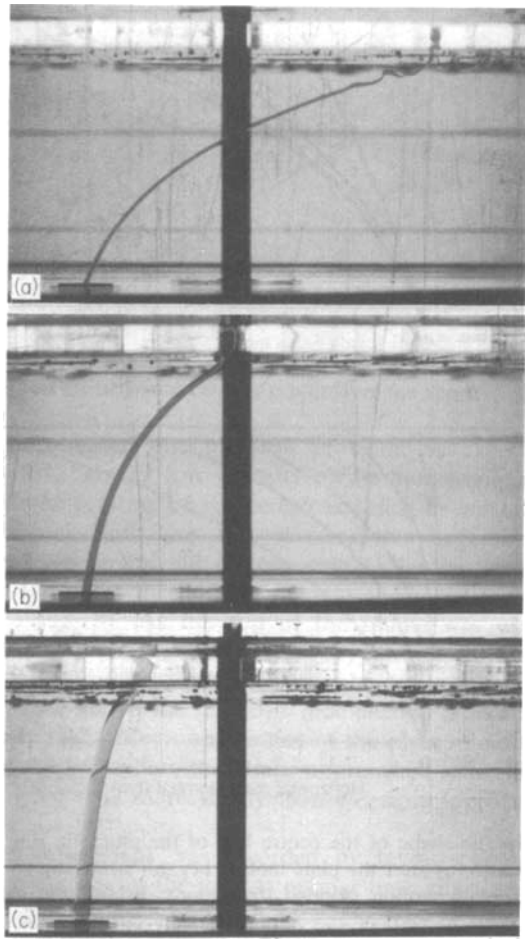

Figure 7. Photographs of the final steady state form of the plumes in the presence of plate motion in runs A1, A2 and A3. The plume is carried from left to right between the viewer and the axial shaft.

since, according to our theory, we could take any point along the plume trajectory to be a virtual source. More explicitly, if we take the virtual source to be at height z_0 and define the x coordinate of the plume to be zero at this height, then (4) becomes

$$x(z) = k'(z^2 - z_0^2). \tag{15}$$

For N data points along the plume profile, we obtain the least squares estimate for k' (and thus k)

$$\hat{k} = \frac{\sum_{i=1}^{N} x_i(z_i^2 - z_0^2)}{\sum_{i=1}^{N} (z_i^2 - z_0^2)^2} \tag{16}$$

and we model

$$\hat{x}_i = \hat{k}(z_i^2 - z_0^2). \tag{17}$$

Figure 8 shows the steady-state plume profiles $x(z)$ and the least-squares fits $\hat{x}$ for all experiments. The plume profiles are described quite adequately by the best-fit parabolas. However, in order to confirm our initial hypothesis, it is necessary to show that the resulting estimates for k are independent of the experimental plume parameters ($\Delta\rho$, a, η_{plume}). Note that (16) can be applied to estimate k' for any maximum number of data points N, hence any cut-off height in the box. By varying this

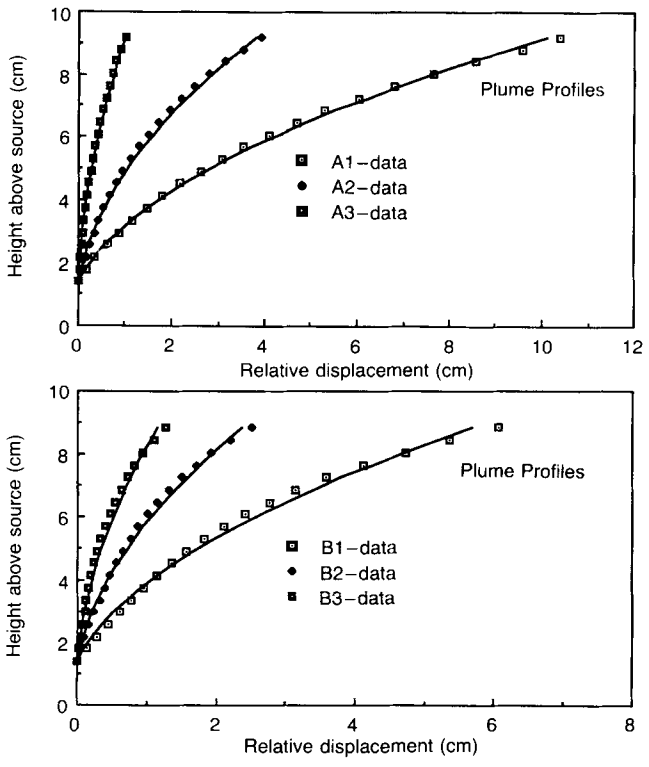

Figure 8. The measured steady state plume profiles in the presence of plate motion and the parabolas fitted using the least-squares method. The lid lies at a height of 10.5 cm from the base in (a) and at 9.5 cm in (b). Data from close to the lid are omitted because the rise of the plume there is influenced by proximity to the holes in the lid. Horizontal displacement is relative to the plume position at a height 1.4 cm from the base.

maximum height for which the parabolic fit is obtained, we gain some further idea as to how appropriate the parabolic curves really are. In Fig. 9 we show values of k determined as a function of cut-off height for the fit. The estimates level off above about 4 cm and give an average value of $k = 0.54 \pm 0.02$. One notable exception is experiment A1 in which estimates for k are systematically a factor of about 30 per cent higher than for the other experiments. We believe this one anomaly results from inaccuracy in the determination of the exceptionally small plume radius in that experiment. Estimates for k are inversely proportional to

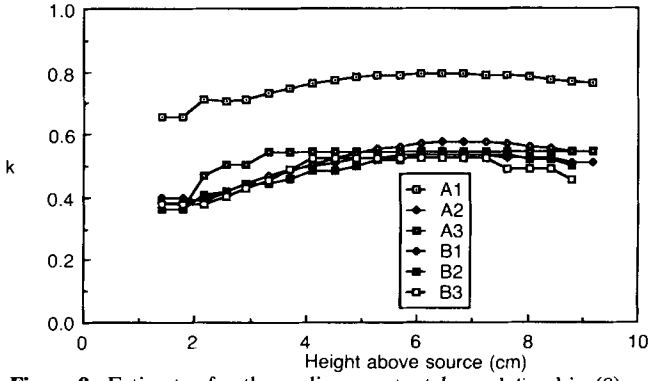

Figure 9. Estimates for the scaling constant k, as defined in (8), as functions of the maximum height used in the parabolic fit for six experiments. Only experiment A1 gives estimates significantly different from one fixed value, and this difference can be attributed to a small error in measurement of the plume diameter.

the square of the plume radius, a^2, and an underestimate of the diameter $2a$ by only 0.15 mm in experiment A1 could explain the discrepancy seen in Fig. 9. As discussed above, measurement errors of order ± 0.3 mm in the diameter are expected. The other experiments, having larger radii, are not so susceptible to this source of error. Furthermore, the results for A1 show an almost constant estimate for k as a function of maximum height, so we are confident that the plume behaviour is not significantly different from the other plumes.

The similarity of all the estimates for k in Fig. 9 confirm the original hypothesis that each plume element trajectory can be described in terms of a modified Stokes velocity. The value of k does not depend upon the plume radius, density anomaly or viscosity contrast. It increases slightly, perhaps, with height, noting that the angle of inclination of the plume increases with height, but we find no dependence of k upon the magnitude of maximum deflection, which varies greatly between experiments. Note from Fig. 8 that plume deflection increases slightly faster than z^2 near the top of the tank. This is expected, since the rigid upper plate will retard the conduit rise within several conduit diameters of the plate: our theoretical model is not applicable immediately beneath the plate, but this is not a serious restriction in applications to the Earth.

The time evolution of the horizontal displacement is shown for each experimental plume in Figs 10(a–f). The displacement was measured as a function of time at three almost equally spaced heights in the tank (3.8 cm, 5.7 cm, and 7.7 cm above the bottom of the tank). At time zero, the plate motion is turned on and the plume begins to stretch. At a later time plate motion is turned off and the plume relaxes.

Equations (12) and (13) above predict the time evolution at each height for the simple shear flow, and theoretical

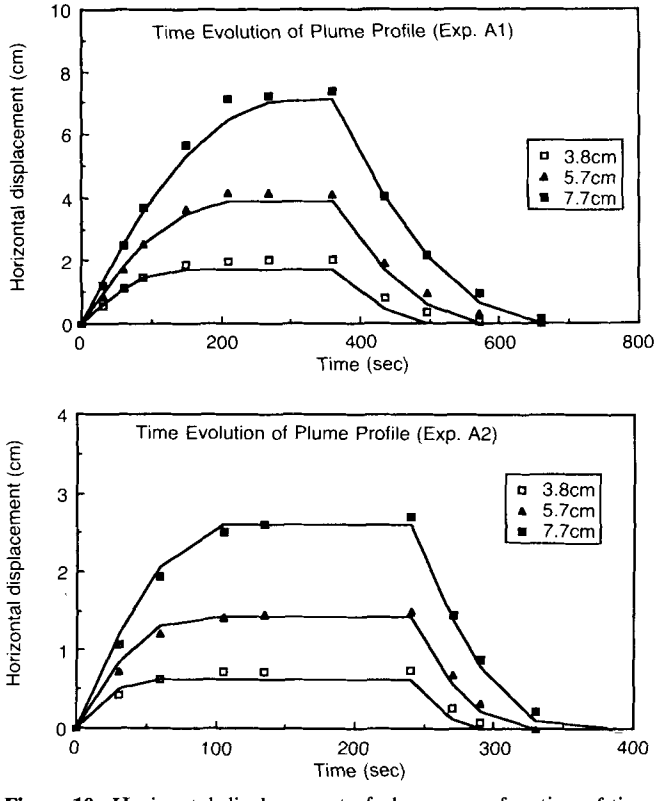

Figure 10. Horizontal displacement of plumes as a function of time in each experiment. The symbols give the time history at heights 3.8 cm, 5.7 cm, and 7.7 cm above the bottom of the tank. The solid curves are theoretical predictions based on the previous, empirical determinations of k from steady-state plume shapes.

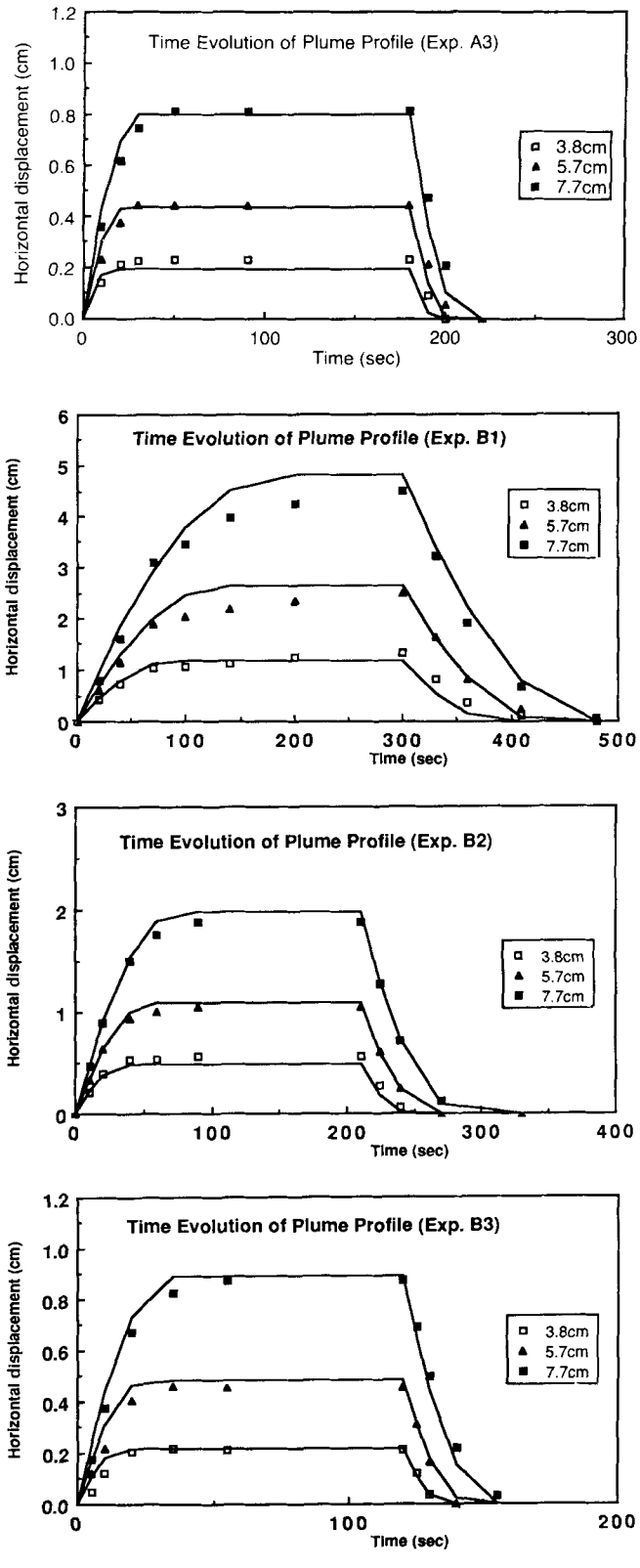

Figure 10. (*continued*)

values based on these expressions are shown as solid lines in Fig. 10. These curves are calculated for the single best-fit value of k determined in each experiment. The relaxation parts of the curves fit a little better than the stretching parts, but the agreement is quite good in both cases. We conclude that our initial hypothesis, equation (1), predicts the approximate time evolution of a plume conduit in a shear flow in addition to its steady-state profile.

DISCUSSION

We have shown that the shapes of plume conduits formed from a continuous, fixed flux of buoyant fluid in a simple shear flow are determined by the sum of the horizontal advection by the surrounding fluid and a constant velocity of rise for individual plume elements. This vertical velocity can be expressed as a modified Stokes velocity which scales as the square of the plume radius times the density contrast. The modified Stokes velocity is shown to depend only weakly, if at all, on the angle of inclination of the plume to the vertical.

The numerical constant for the Stokes law scaling is $k = 0.54 \pm 0.02$, which is close to twice that for the motion of a sphere ($k = 0.33$). This is reasonable, since each plume element is actually a segment of a cylindrical conduit, and since the Stokes constant for a cylinder is always larger than that for a sphere. We cannot fully justify the fact that k is approximately constant regardless of plume deflection or inclination. Our initial hypothesis resulted not from theoretical considerations, but sprang largely from the observation that a steady plume in a simple shear flow is bent into a simple parabolic shape.

In their treatment of conduit instability, Skilbeck & Whitehead (1978) used the formula for the rise of an inclined, rigid cylinder to approximate the rise velocity of plume elements

$$v_s = \log\left(\frac{l}{a}\right)\frac{ga^2\,\Delta\rho}{8\eta}\frac{(3-\cos 2\theta)}{(\sin\theta)^{1/2}}, \tag{18}$$

where l/a is a 'reasonable' cylinder length to radius ratio and θ is the conduit inclination to the horizontal. (The factor $1/(\sin\theta)^{1/2}$ is included to account for the change in plume radius with inclination.) They *assumed* that $l/a \approx 10$ which, for a weakly deflected plume ($\theta \approx 90°$) implies that

$$v \approx 1.15\frac{ga^2\,\Delta\rho}{\eta}, \tag{19}$$

i.e. $k = 1.15$. According to our experiments this is incorrect by more than a factor of 2. Since the θ-dependent factor in equation (18) varies by only 13 per cent for $30° < \theta < 90°$, we might improve (18) by simply choosing a 'correct' value for l/a, namely $l/a \approx 2.9$. However, this is a completely *ad hoc* remedy which contains no more of the physics of the problem than equation (1).

Although (18) accounts for the effect of inclination on the rise of a rigid cylinder, there is no reason to believe that the appropriate value of l/a should remain constant. The fact that l/a enters (18) logarithmically and the weak θ-dependence do suggest that the effective value for k in (1) may change very little with conduit inclination. We note, however, that (18) predicts a small decrease in k with increasing deflection where, if anything, our experiments suggest a small increase.

Of course, we have shown only that (1) *approximates* plume trajectories; the fits to data and the constancy of k are not perfect. The above discussion is not intended as a criticism of Skilbeck and Whitehead, but we wish to emphasize the following points: our hypothesis [equation (1)] describes quite accurately the deflection of low viscosity plumes and this description should be adequate for studying the deflection of stable plumes in the mantle. Equation (1) has the merit of great simplicity which is very helpful in understanding the evolution of plumes responding to changing mantle flow and plate motions. We have no theoretical reason to believe that (1) is exact or that any similar exact expression exists. For this reason we have not included an exhaustive discussion of the fit between data and theory: the simple theory is clearly a good approximation over a wide range of conditions. In applications to mantle plumes, other first-order uncertainties, such as the ambient mantle viscosity structure, are likely to be more important than any inadequacies of our simple theory for plume deflection.

One additional observation made during our laboratory experiments but not previously noted is worth a mention here. Along the axis of the plume above a height of two to four centimetres from the source there appeared a thin vertical stripe of non-dyed fluid from outside the plume. This stripe became even more clearly visible when the plume was laid down beneath the rigid lid and began to spread horizontally. The stripe indicates a bifurcation of the flow within the plume, from a simple nearly vertical flow near the source (this flow would exist along the whole length of vertical plumes) to a cylindrical vortex at positions where the plume axis is inclined to the vertical. The cylindrical vortex involves two oppositely directed recirculating eddies with axes parallel to the plume axis and is a natural corollary to our description of the rise of the plume conduit according to a modified Stokes velocity (a similar but spherical vortex occurs in a rising sphere). The entrainment of surrounding, non-dyed fluid into the conduit may be a result of viscous stresses, or may result from molecular diffusion of water out of the dyed plume fluid, making buoyant a small amount of outer fluid (Griffiths 1986a,b). This cylindrical vortex flow is superimposed on the relatively rapid flow of buoyant material upward along the conduit.

Our experiments involve chemical plumes only, and it is wise to consider the extent to which these will model thermal plumes in the mantle. In a thermal plume, conduction of heat has the potential to influence the density and viscosity structure. Indeed, for vertical plumes in a stationary environment, the coupling of purely axial flow with purely radial (horizontal) conduction of heat will generate profiles of temperature, density anomaly and vertical velocity which all decrease with distance from the plume axis. Viscosity is strongly dependent on temperature and increases with radial distance. However, in a tilted plume radial diffusion of heat is coupled to the internal recirculation of the cylindrical vortex, as well as to the axial flow. This coupling previously has been discussed for the case of the spherical vortex which is generated in a rising diapir (Griffiths 1986a,b). For large Peclet number the vortex circulation maintains an approximately uniform

temperature throughout a diapir and temperature gradients resulting from conduction are confined to a very thin boundary layer around the edge of the diapir. A diapir slowly enlarges and cools as it rises and entrains surrounding material. For a tilted conduit the Peclet number based on the modified Stokes velocity will again be large (assuming radii greater than 1 km). Furthermore, the relatively rapid axial flow will maintain a close communication with the plume source. Hence diffusion of heat is likely to have only small effects on the temperature, viscosity and density structure of the plume. The conduit's rise through the mantle and the associated cylindrical vortex also imply that an extensive thermal halo such as that around a vertical plume in a stationary environment cannot develop and any temperature gradients within the plume will be limited.

We conclude this paper by considering two general examples of stable plumes interacting with mantle shear flow. These simple models illustrate the usefulness of (1) in understanding mantle plumes.

Simple shear flow with layered viscosity

Consider a simple shear flow driven by an upper plate having velocity u_0, with a rigid bottom as shown in Fig. 11(a). Also, let the bottom part of the fluid ($0 \le z \le fh$) have viscosity η_1, and the upper part ($fh < z < h$) have viscosity η_2. If $\eta_1 > \eta_2$, the horizontal velocity profile $u(z)$ will be as illustrated in Fig. 11(a). Using analytical expressions obtained for $u(z)$, it is easy to show using (5) that a steady plume injected at the bottom of the fluid will have a trajectory given by

$$x(z) = \frac{\eta_2}{kg\,\Delta\rho a^2}\frac{u_0}{h}\frac{z^2}{2}\left[\frac{1}{f+\frac{\eta_1}{\eta_2}}(1-f)\right]. \tag{20}$$

The trajectory (20) is the same as the uniform viscosity case except for the constant factor in brackets. Thus, the plume trajectory remains parabolic. This shape will occur whenever *shear stress* is constant throughout the depth of the fluid. Another way to look at this result is that both the horizontal force acting on the conduit and the vertical force, or drag, resisting the rise of the conduit are proportional to the local background fluid viscosity. We conclude that, at least for this simple case, it is the shear stress applied at the surface by the moving plate that determines the plume deflection and the vertical structure does not alter the shape of the trajectory. We note here that we have assumed that the plume radius remains constant with height. As long as the plume viscosity is much less than the surrounding fluid viscosity this will be approximately correct (see Richards, Hagar & Sleep 1987).

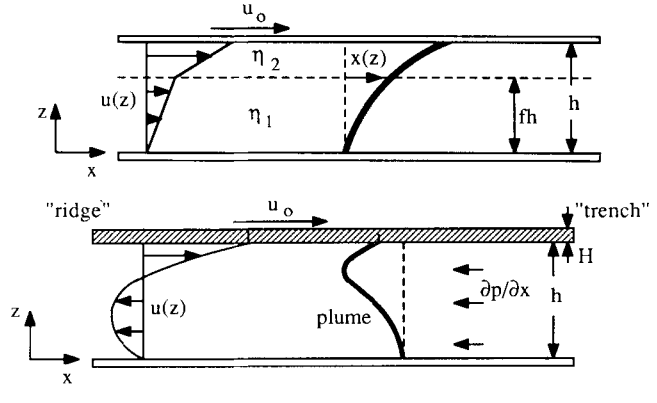

Figure 11. (a) Diagram of plume deflection in a plate-driven shear flow with vertical viscosity stratification. (b) Diagram of plume deflection in a simple return flow model.

Simple return flow (uniform viscosity)

Flow in the mantle due to plate motions and, perhaps, other modes of convection must involve a return flow component such that there is little or no net horizontal advection of mantle material. In the case of Hawaii and other Pacific hotspots, there must be a large component of return flow directly to the East Pacific Rise owing to the size of the Pacific plate subduction and its large spreading and subduction rates (Hager & O'Connell 1981). Here we calculate the trajectory of a plume in a very simple return flow model.

Figure 11(b) illustrates the return flow model. Again, the moving lithospheric plate, of thickness H, drives flow in the mantle below, but we require a return flow such that no net mass flux occurs through a vertical section. Here we take the mantle, or at least that part of it involved in plate-driven flow, to be of uniform viscosity η and thickness h. The flow can be modelled as being driven by a uniform pressure gradient, $\frac{\partial p}{\partial x}$, driving material back toward the spreading ridge from the trench or subduction zone. We have used a rigid bottom boundary to serve as a 'fixed' plume source.

The velocity profile (see e.g. Turcotte & Schubert 1982) is given by

$$u(z) = u_0\left(\frac{z}{h}\right)\left[1 + 6\left(\frac{H}{h}+\frac{1}{2}\right)\left(\frac{z}{h}-1\right)\right]. \tag{21}$$

Using (5), the plume trajectory is given by

$$x(z) = \frac{u_0}{v_s}\left[\frac{z^2}{2h} + 6\left(\frac{H}{h}+\frac{1}{2}\right)\left(\frac{z^3}{3h^2}-\frac{z^2}{2h}\right)\right]. \tag{22}$$

The shape of this trajectory is also shown in Fig. 11(b) for the case $H/h = 1/6$, which corresponds to a return flow confined to the upper mantle. The most negative horizontal excursion of the plume occurs at

$$\frac{z_{max}}{h} = 1 - \frac{1}{6\left(\frac{H}{h}+\frac{1}{2}\right)}. \tag{23}$$

In Table 2 we show the maximum horizontal excursion $x(z_{max})$ and the surface (hotspot) excursion $x(h)$ with respect to the plume source for three different values of H/h. Results are given for return flow confined to a shallow low viscosity channel, to the upper mantle and to the whole depth of the mantle. The previous example with viscosity stratification, which demonstrates that shear stress rather than viscosity is important, shows that the low viscosity channel case is probably not meaningful, unless convection associated with plate motion is strictly confined to this 'decoupling' channel.

Table 2. Predicted characteristics of plumes in various return flow models for the mantle.

	H/h	z_{max}/h	$x(z_{max})$	x(h) [surface]
low viscosity channel	1/2	.83	$-.58\frac{u_0}{v_s}h$	$-.5\frac{u_0}{v_s}h$
upper mantle	1/6	.75	$-.28\frac{u_0}{v_s}h$	$-.17\frac{u_0}{v_s}h$
whole mantle	1/29	.69	$-.17\frac{u_0}{v_s}h$	$-.03\frac{u_0}{v_s}h$

First, we note from (23) and Table 2 that the height z_{max} is quite a large fraction of the layer depth h. Thus, as illustrated in Fig. 11(b), the maximum excursion $x(z_{max})$ occurs near the top of the layer. We also note that the difference between this maximum excursion and the surface hotspot position is small for the case of upper mantle recirculation. For all of the cases considered, the surface hotspot position is the result of a plume bent over from its source in the *opposite* direction to the plate motion.

We conclude this example by estimating $x(z_{max})$ for some possible combinations of mantle and plume parameters. If we let the plume radius be $a = 70$ km, the density contrast $\Delta\rho = 0.05$ g/cm^3, and the mantle viscosity $\eta = 10^{22}P$, then we find from (1) $v_s = 5$ cm/yr. If the plate velocity is $u_0 = 10$ cm/yr then we obtain $x(z_{max}) = 350$ km for upper mantle return flow and $x(z_{max}) = 1000$ km for whole mantle return flow. The corresponding surface positions will be 210 km and 180 km, respectively, from the source. The plume radius value of $a = 70$ km may at first thought seem quite large. However, if the *uppermost* mantle has a viscosity as small as $\sim 10^{20}P$, a plume radius an order of magnitude smaller would lead to the same deflection. These numerical examples are not intended as actual estimates for any particular mantle plume, but only to show that modestly deflected and stable plumes are within the range of reasonable parameter choices.

As a prelude to a discussion of the behaviour of specific mantle plumes (paper in preparation), we point out that a horizontal plume excursion of as much as half of the upper mantle depth appears to be precluded by the sharpness of the bend in the Hawaiian–Emperor seamount chain. Since each plume element behaves like an independent Stokeslet, a change in the direction of plate motion leaves the old plume trajectory 'stranded' in horizontal position. Noting again that the maximum excursion occurs very near the base of the lithosphere, the join between the steady-state plume tracks before and after the change in plate motion would be expected to show a radius of curvature comparable to the maximum horizontal change in the plume trajectory.

The range of applications of (1) in understanding mantle plumes and hotspots is potentially large. Most researchers have tended to concentrate on the Hawaii hotspot, but other hotspot tracks may be just as interesting. Sufficiently weak mantle plumes may be deflected so far as to be unstable in the manner demonstrated by Whitehead (1982). The surface expression of these weak plumes (which will generate only small seafloor swells) are likely to show stronger evidence for episodicity, resulting from instability, in volcanism and lithospheric heating. Although our description of plume trajectories is only approximate, it does show that various effects due to mantle flow and plate motions are not, fundamentally, very complicated.

ACKNOWLEDGMENTS

We thank Derek Corrigan for construction of the laboratory tank, and Ross Wylde-Browne for photographic work. Discussions with Geoff Davies were most enlightening. Mark Richards acknowledges travel support from the University of Oregon Office of Research.

REFERENCES

Griffiths, R. W., 1986a. Thermals in extremely viscous fluids, including the effects of temperature-dependent viscosity, *J. Fluid Mech.*, **166,** 115–138.

Griffiths, R. W., 1986b. The dynamics of mantle thermals with constant buoyancy or anomalous internal heating, *Earth planet. Sci. Lett.*, **78,** 435–446.

Griffiths, R. W., Gurnis, M. & Eitelberg, G., 1988. Holographic measurements of surface topography in laboratory models of mantle hotspots, submitted to *Geophys. J.*

Hager, B. H. & O'Connell, R. J., 1981. A simple global model of plate dynamics and mantle convection, *J. geophys. Res.*, **86,** 4843–4867.

Molnar, P. & Stock, J., 1987. Relative motions of hotspots in the Pacific, Atlantic and Indian Oceans since late Cretaceous time, *Nature,* **327,** 587–591.

Morgan, W. J., 1972. Plate motions and deep mantle convection, *Mem. geol. Soc. Am.*, **132,** 7–22.

Morgan, W. J., 1982. Hotspot tracks and the opening of the Atlantic and Indian Oceans, in *The Sea,* vol. 10, ed. Emiliani, C., Wiley, New York.

Olson, P. & Nam, I. S., 1986. Formation of seafloor swells by mantle plumes, *J. geophys. Res.*, **91,** 7181–7191.

Olson, P. & Singer, H. A., 1985. Creeping plumes, *J. Fluid Mech.*, **158,** 511–531.

Poreda, R., Craig, H. & Schilling, J. G., 1980. ^{3}He/^{4}He variations along the Reykjanes Ridge, *Eos, Trans. Am. geophys. Un.*, **61,** 1158.

Richards, M. A., Hagar, B. H. & Sleep, N. H., 1988. Dynamically supported geoid highs over hotspots, *J. geophys. Res.*, in press.

Skilbeck, J. N. & Whitehead, J. A., 1978. Formation of discrete islands in linear chains, *Nature,* **272,** 499–501.

Turcotte, D. L. & Schubert, G., 1982. *Geodynamics: Applications of Continuum Physics to Geological Problems,* New York, Wiley, 450 pp.

Whitehead, J. A., 1982. Instabilities of fluid conduits in a flowing Earth—are plates lubricated by the asthenosphere?, *Geophys. J. R. astr. Soc.*, **70,** 415–433.